nature publishing group

Downregulating SOCS3 with siRNA ameliorates insulin signaling and glucose metabolism in hepatocytes of IUGR rats with catch-up growth

Juan Ye[1], Ruidan Zheng[1], Qun Wang[1], Lihong Liao[1], Yanqin Ying[1], Huiling Lu[1], Katherine Cianflone[2], Qin Ning[1] and Xiaoping Luo[1]

BACKGROUND: Individuals with intrauterine growth retardation (IUGR) who demonstrate a catch-up in body weight are prone to insulin resistance. High expressions of suppressor of cytokine signaling 3 (SOCS3) are thought to aggravate insulin resistance. We hypothesized that downregulating SOCS3 expression via small interfering RNA (siRNA) might have beneficial effects on insulin-resistant hepatocytes of catch-up growth IUGR rats (CG-IUGRs).

METHODS: An IUGR rat model was employed via maternal nutritional restriction. After evaluating metabolic states of CG-IUGR offspring, effective *SOCS3*-specific siRNA (siSOCS3) was transfected into cultured hepatocytes using liposomes. mRNA levels of SOCS3, insulin receptor substrates (IRSs), phosphatidylinositol 3-kinase (PI3K), and Akt2, key gluconeogenesis genes, were assessed via real-time PCR. Protein expression and phosphorylation changes were evaluated via western blot.

RESULTS: CG-IUGR hepatocytes showed increases in SOCS3 and gluconeogenic gene expressions, and decreases in IRS1 and PI3K expressions as compared with controls. After transfecting CG-IUGR hepatocytes with siSOCS3, protein levels of IRS1, PI3K, and phosphorylated Akt2 were higher as compared with those of untransfected CG-IUGR cells. Transcriptional suppression effects of gluconeogenesis genes were more obvious in siSOCS3-treated cells after insulin stimulation.

CONCLUSION: Additional insights were provided to understand mechanisms of insulin resistance in CG-IUGR rats. Downregulating SOCS3 might improve insulin signaling transduction and ameliorate hepatic glucose metabolism in insulin-resistant CG-IUGR rats *in vitro*.

Worldwide epidemiological data have shown that intrauterine growth retardation (IUGR), low birth weight, and subsequent adulthood obesity are highly correlated with the development of metabolic syndrome, which comprises hypertension, cardiovascular disease, type 2 diabetes mellitus, and dyslipidemia. Insulin resistance is considered to be a fundamental contributor to metabolic syndrome (1–3). The underlying causes of IUGR are complicated. In developed countries, poor placental function and cigarette smoking during pregnancy are the most common factors causing IUGR, although maternal malnutrition is the major determinant of IUGR in developing countries (4). Approximately 85–90% of infants with IUGR demonstrate catch-up growth during the first 2 y, and those who display a catch-up in body weight are more prone to insulin resistance (5). However, the underlying molecular mechanisms that result in insulin resistance in individuals with catch-up IUGR are still not fully understood.

Suppressor of cytokine signaling (SOCS)-family proteins have been identified as inhibitors of cytokine-induced signaling pathways in various tissues and serve as physiological regulatory feedback loops (6). Suppressor of cytokine signaling 3 (SOCS3) is highly expressed in the liver, skeletal muscle, and adipose tissue of animal models with insulin resistance (7,8). Studies have also shown that SOCS3 plays an important role in regulating insulin signaling in several ways. It can bind the insulin receptor (IR), impair the phosphorylation of the insulin receptor substrate (IRS)1 and 2 without inhibiting IR phosphorylation, and reduce the expression of IRS1 and IRS2 via a ubiquitin-mediated degradation (9). Furthermore, the overexpression of SOCS3 can also inhibit preproinsulin gene transcription in pancreatic β-cells, which directly reduces insulin secretion (10). Heterozygous *SOCS3*-deficient mice do not develop insulin resistance when exposed to a high-fat diet (11), whereas a *SOCS3* deletion causes embryonic lethality on days 12–16 (12). Therefore, tissue- or cell-specific knockouts/knockdowns of *SOCS3* were developed in recent studies. Liver-specific *SOCS3* knockout mice demonstrated an apparently improved insulin sensitivity in the liver but exhibited obesity and systemic insulin resistance with age (13). A *SOCS3* knockdown increased fatty acid oxidation in primary adipocytes of rats with diet-induced obesity (14). Our previous study confirmed that downregulation of SOCS3 promoted an insulin-stimulated glucose transporter 4 translocation and ameliorated insulin sensitivity in IUGR skeletal muscle cells (15). Although studies concerning the role of SOCS3 in insulin signaling have been extensively performed both *in vitro* and *in vivo*, and primarily focused on using adipose tissue, skeletal muscle,

[1]Department of Pediatrics, Tongji Hospital, Tongji Medical College, Huazhong University of Science and Technology, Wuhan, China; [2]Centre de Recherche Institut Universitaire de Cardiologie et Pneumologie de Québec, Université Laval, Québec City, Québec, Canada. Correspondence: Xiaoping Luo (xpluo@tjh.tjmu.edu.cn)

Received 29 December 2011; accepted 30 June 2012; advance online publication 14 November 2012. doi:10.1038/pr.2012.123

Table 1. Comparison of biometry of AGA and CG-IUGR offspring from birth to 8 wk of age

	Body weight (g)		Body length (cm)		BMI (kg/m^2)	
Age (wk)	AGA ($n = 24$)	CG-IUGR ($n = 23$)	AGA ($n = 24$)	CG-IUGR ($n = 23$)	AGA ($n = 24$)	CG-IUGR ($n = 23$)
0	5.93 ± 0.35	4.48 ± 0.29*	4.87 ± 0.14	4.54 ± 0.10*	2.51 ± 0.11	2.17 ± 0.08*
1	16.72 ± 1.18	13.70 ± 1.67*	7.16 ± 0.26	6.81 ± 0.20*	3.25 ± 0.19	2.99 ± 0.22*
2	29.19 ± 2.06	32.18 ± 4.42*	9.22 ± 0.36	9.03 ± 0.51*	3.44 ± 0.20	3.97 ± 0.44*
3	49.84 ± 4.30	56.18 ± 3.40*	11.63 ± 0.51	11.40 ± 0.35	3.71 ± 0.24	4.31 ± 0.21*
4	68.81 ± 4.64	78.23 ± 5.02*	14.55 ± 0.58	14.00 ± 0.79	3.26 ± 0.22	3.96 ± 0.32*
5	97.86 ± 5.89	114.75 ± 6.52*	15.95 ± 0.64	15.68 ± 0.72	3.84 ± 0.45	4.70 ± 0.59*
6	123.72 ± 7.73	147.89 ± 10.22*	17.08 ± 0.56	16.87 ± 0.66	4.24 ± 0.44	5.22 ± 0.63*
7	148.22 ± 8.79	179.76 ± 12.07*	18.13 ± 0.63	17.85 ± 0.75	4.44 ± 0.47	5.66 ± 0.70*
8	157.27 ± 11.83	196.88 ± 14.89*	19.08 ± 1.09	18.45 ± 1.16	4.41 ± 0.39	5.59 ± 0.62*

Data are presented as mean ± SD.

AGA, appropriate for gestational age; CG-IUGR, catch-up growth intrauterine growth retardation rats.

*$P < 0.05$ vs. AGA rats at the same age.

liver, or cell lines, research on the role of SOCS3 in the insulin signaling of primary hepatocytes of IUGR offspring exhibiting early catch-up growth is rare.

In this study, we assessed basal and insulin-stimulated expressions of SOCS3, IRS1, IRS2, phosphatidylinositol 3-kinase (PI3K), and Akt2 in the hepatocytes of IUGR rats undergoing an early catch-up in body weight, as well as in those of normal rats. Small interfering RNAs (siRNAs) targeting *SOCS3* were designed and evaluated for their gene-silencing effects in hepatocytes with insulin resistance. We demonstrated that a downregulation of SOCS3 can ameliorate insulin resistance of catch-up IUGR rats *in vitro* by enhancing the signal transduction of the post-insulin receptor pathway.

RESULTS

Early Catch-Up Growth IUGR Model

The birth weights of the pups with IUGR were lower than those of the appropriate for gestational age (AGA) pups. The pups with IUGR demonstrated an accelerated weight gain from postnatal week 1 and caught up with the AGA pups before the third postnatal week. After that, the weights of the pups with IUGR were significantly higher and kept increasing above those of the AGA pups. The birth lengths of the pups with IUGR were lower than those of the AGA pups. The pups with IUGR demonstrated a trend toward a gradual catch-up in body length after birth and had caught up to the AGA group by the third postnatal week. The BMIs of the pups with IUGR were lower than those of the AGA pups before 2 wk of age, but gradually surpassed the AGA pups thereafter (**Table 1**).

At 8 wk, both absolute growth rate and fractional growth rate of the catch-up growth IUGR rats (CG-IUGRs) were significantly higher than those of AGA rats ($P < 0.05$). The liver weight per body weight and liver weight per body length were higher in CG-IUGR group as compared with the AGA group, but the differences did not reach statistical significance ($P > 0.05$), whereas the fat mass per body weight and fat mass per body length were statistically higher in CG-IUGR than AGA rats ($P < 0.05$). There was no difference in the skeletal muscle weight per body weight of CG-IUGR rats as compared to AGA rats. However, statistical difference existed in the skeletal muscle weight per body length between these two groups (**Table 2**).

Table 2. Composition of organ masses and growth rates in 8-wk-old offspring

	AGA	CG-IUGR
Liver		
Liver weight (% body weight)	3.91 ± 0.40	4.14 ± 0.37
Liver weight (% body length)	38.99 ± 6.02	46.72 ± 9.70
Skeletal muscle		
Muscle weight (% body weight)	2.51 ± 0.24	2.70 ± 0.10
Muscle weight (% body length)	25.20 ± 4.87	30.15 ± 3.70*
Fat pads		
Fat mass (% body weight)	0.51 ± 0.24	0.88 ± 0.16*
Fat mass (% body length)	5.02 ± 2.17	9.79 ± 2.21*
Growth rate		
AGR (g/day)	2.63 ± 0.48	3.44 ± 0.56*
FGR (g/day/g)	0.42 ± 0.08	0.78 ± 0.15*

Numbers per group for composition of organ masses: $n = 8$. Numbers per group for growth rate: AGA, $n = 24$; CG-IUGR, $n = 23$. Data are presented as mean ± SD.

AGA, appropriate for gestational age; AGR, absolute growth rate; CG-IUGR, catch-up growth intrauterine growth retardation rats; FGR, fractional growth rate.

*$P < 0.05$ vs. AGA.

Glucose and Lipid Metabolism

There were no significant differences in fasting glucose levels of CG-IUGR rats as compared with the AGA rats (5.18 ± 0.47 mmol/l vs. 4.82 ± 0.76 mmol/l; $P > 0.05$). However, the fasting insulin concentration was higher in CG-IUGR than AGA rats (18.20 ± 5.92 mU/l vs. 10.72 ± 3.31 mU/l; $P < 0.01$). In addition, there were significant differences in the homeostasis model assessment of insulin resistance (4.19 ± 0.36 vs. 2.30 ± 0.34; $P < 0.01$) and high density lipoprotein-cholesterol (0.71 ± 0.17 mmol/l vs. 0.93 ± 0.11 mmol/l; $P < 0.01$) between the CG-IUGR and AGA groups, respectively, whereas there were

Table 3. Glucose levels (mmol/l) and insulin levels (mIU/l) assessed via an IPGTT in 8-wk-old offspring

Group		0 min	30 min	60 min	90 min	120 min
AGA	Glucose	4.91 ± 0.20	6.47 ± 1.11	5.26 ± 0.32	4.23 ± 0.11	4.29 ± 0.10
	Insulin	9.72 ± 4.13	20.96 ± 9.30	16.48 ± 7.44	15.27 ± 2.72	9.84 ± 1.99
CG-IUGR	Glucose	5.48 ± 0.64	7.87 ± 0.37*	6.18 ± 0.37*	5.02 ± 0.19*	5.17 ± 0.23*
	Insulin	19.66 ± 6.25*	43.36 ± 13.70*	34.72 ± 14.78*	28.76 ± 6.39*	22.54 ± 4.06*

Data are presented as mean ± SD ($n = 6$).

AGA, appropriate for gestational age; CG-IUGR, catch-up growth intrauterine growth retardation rats; IPGTT, intraperitoneal glucose tolerance test.

*$P < 0.05$ vs. AGA.

no differences in low density lipoprotein-cholesterol (1.48 ± 0.29 vs. 1.57 ± 0.36; $P > 0.05$), triglyceride (0.88 ± 0.36 mmol/l vs. 0.78 ± 0.16 mmol/l; $P > 0.05$), total cholesterol (2.75 ± 0.38 vs. 2.96 ± 0.32; $P > 0.05$), and free fatty acid (247.12 ± 85.53 vs. 208.83 ± 51.56 μmol/l; $P > 0.05$) levels.

Furthermore, using the intraperitoneal glucose tolerance test, it was determined that glucose and insulin levels at 30, 60, 90, and 120 min were higher in CG-IUGR than AGA rats (Table 3).

Increased SOCS3 Expression in Primary Hepatocytes of CG-IUGR Rats

We investigated whether SOCS3 mRNA and protein expression levels were different between these two groups. After 24 h of being in a serum-free culture with or without 100 nmol/l insulin for 30 min, cells were harvested for mRNA expression assessment with real-time PCR and protein level determination via western blotting. As shown in Figure 1, SOCS3 mRNA expression in CG-IUGR hepatocytes was greater than that of the AGA hepatocytes at baseline. Furthermore, increases in SOCS3 expression were more notable in the CG-IUGR hepatocytes after stimulation with insulin, which was consistent with the protein expression levels of SOCS3.

Impaired Insulin Signaling in Primary Hepatocytes of CG-IUGR Rats

The expression levels of molecules involved in the postinsulin receptor pathway were assessed to determine whether there were alterations in the insulin signaling of CG-IUGR hepatocytes as compared with AGA hepatocytes. As shown in Figure 2, the basal mRNA levels of IRS1 ($P < 0.01$, Figure 2a) and PI3K ($P < 0.01$, Figure 2c) were higher in the AGA group than in the CG-IUGR group. After stimulating the cells with insulin, these differences were more obvious between the two groups. Furthermore, there were no statistical differences in basal IRS2 ($P > 0.05$, Figure 2b) or Akt2 ($P > 0.05$, Figure 2d) mRNA expression levels. After treatment with 100 nmol/l insulin, the mRNA expression levels of all molecules were higher than those at basal conditions. The increased expression of Akt2 ($P < 0.05$, Figure 2d) in CG-IUGR hepatocytes was much lower than that of the AGA cells, whereas the increased expression of IRS2 (Figure 2b) was not significantly different between these two groups in the insulin-treated state.

The relative protein expressions of the aforementioned molecules were also detected under basal and insulin-stimulated conditions in these two groups via western blotting. The

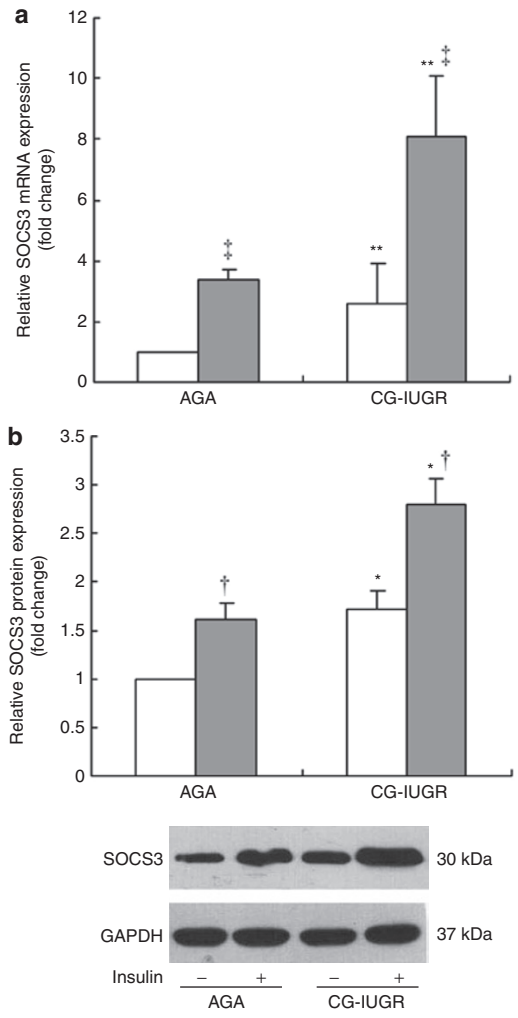

Figure 1. Relative levels of SOCS3 mRNA and protein expression between appropriate for gestational age (AGA) and catch-up growth IUGR rat (CG-IUGR) hepatocytes. (**a**) mRNA level; (**b**) protein level and representative western blots. The gray and white bars refer to with and without insulin treatment, respectively. Data are presented as mean ± SD ($n = 6$). *$P < 0.05$ and **$P < 0.01$ CG-IUGR vs. AGA under the same condition. †$P < 0.05$ and ‡$P < 0.01$ insulin-treated vs. basal condition of the same group. IUGR, intrauterine growth retardation; SOCS3, suppressor of cytokine signaling 3.

decreases in IRS1 (Figure 3a) and phosphorylated Akt2 (Figure 3d) levels in CG-IUGR hepatocytes were more significant under insulin-stimulated conditions, and PI3K p85 concentrations were much lower in the CG-IUGR group than in the AGA group with or without insulin treatment ($P < 0.01$,

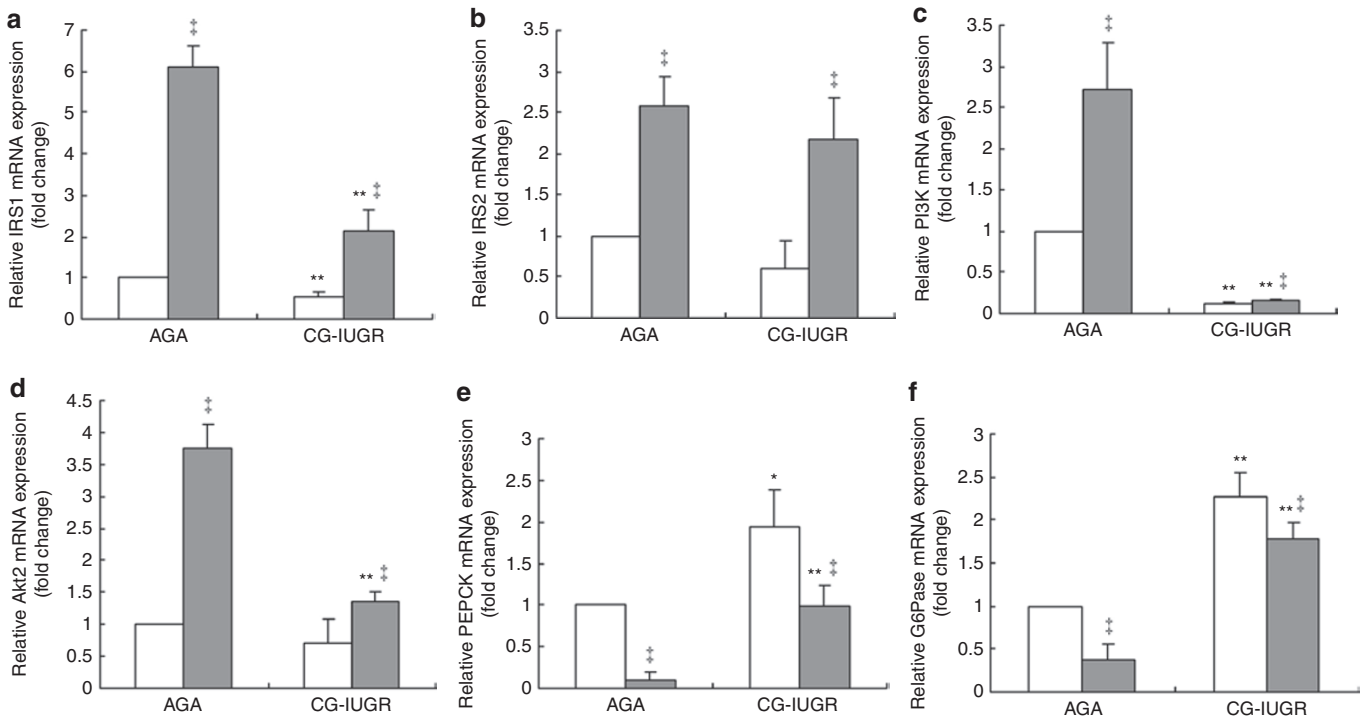

Figure 2. Relative mRNA levels of molecules involved in the downstream signaling of the insulin receptor and relative transcriptional expression of phosphoenolpyruvate carboxykinase (PEPCK) and glucose-6-phosphatase (G6Pase) genes via real-time PCR in appropriate for gestational age (AGA) and catch-up growth IUGR rat (CG-IUGR) hepatocytes. (**a**) IRS1; (**b**) IRS2; (**c**) PI3K; (**d**) Akt2; (**e**) PEPCK; and (**f**) G6Pase. The gray bar refers to insulin treatment, whereas the white bar indicates no insulin treatment. Data are presented as mean ± SD ($n = 6$). *$P < 0.05$ and **$P < 0.01$ CG-IUGR vs. AGA under the same condition. ‡$P < 0.01$ insulin-treated vs. basal condition of the same group. IRS, insulin receptor substrate; IUGR, intrauterine growth retardation; PI3K, phosphatidylinositol 3-kinase.

Figure 3c). However, no decrease in IRS2 protein was obvious between these two groups with or without insulin treatment (Figure 3b).

Altered Transcriptional Expressions of Gluconeogenesis Genes in CG-IUGR Hepatocytes

To evaluate glucose metabolism in CG-IUGR hepatocytes, mRNA levels of phosphoenolpyruvate carboxykinase (PEPCK) and glucose-6-phosphatase (G6Pase) were assessed in liver cells. The transcriptional levels of both PEPCK and G6Pase genes were higher in CG-IUGR than AGA hepatocytes in the basal condition, and decreased in both groups after insulin stimulation; however, the suppressing effects of insulin were more obvious in the AGA group, suggesting that the actions of insulin were blunted in CG-IUGR cells (Figure 2e,f).

Knockdown of SOCS3 Expression by *SOCS3*-siRNA in Primary Hepatocytes

Three siRNAs targeting *SOCS3* and scrambled siRNA were transfected into the primary hepatocytes using the Lipofectamine 2000 reagent (Invitrogen, Carlsbad, CA) to identify the most effective siRNA duplex. Forty-eight hours after siRNA delivery, SOCS3 mRNA and protein were detected via real-time PCR and western blot. The scrambled siRNA did not affect the expression levels of SOCS3, and of the three siRNA duplexes, *SOCS3*-specific siRNA (siSOCS3)-2 displayed the most efficiency in decreasing both mRNA and protein expression of SOCS3 in hepatocytes (Figure 4). These results indicate that siSOCS3-2 is the most efficient duplex for knocking down SOCS3 expression in liver cells, and this siRNA duplex was subsequently delivered in the following experiments.

Downregulation of SOCS3 Expression Ameliorates Insulin Signaling in Hepatocytes of CG-IUGR Rats

Based on the aforementioned differences between AGA and CG-IUGR rats, we chose to determine IRS1 and PI3Kp85 subunit expression after siSOCS3 transfection to evaluate the influences of downregulating SOCS3 on the insulin signal pathway. After 48 h of transfection, the protein levels of IRS1 ($P < 0.05$, Figure 5a) and PI3kp85 ($P < 0.05$, Figure 5b) were increased in hepatocytes isolated from CG-IUGR rats both in the basal and insulin-treated conditions. The expression of phosphorylated Akt2 was higher in the siSOCS3-transfected cells as compared with those that were not transfected, and the augmenting effects were significant after insulin stimulation for 30 min (Figure 5c). These results suggest that insulin signaling was enhanced after knocking down the expression of SOCS3.

Downregulation of SOCS3 Expression Improves Glucose Metabolism in Hepatocytes of CG-IUGR Rats

To investigate the influences of downregulating SOCS3 expression on glucose metabolism in CG-IUGR hepatocytes, the transcriptional levels of PEPCK and G6Pase were compared between siSOCS3-treated and siSOCS3-untreated CG-IUGR

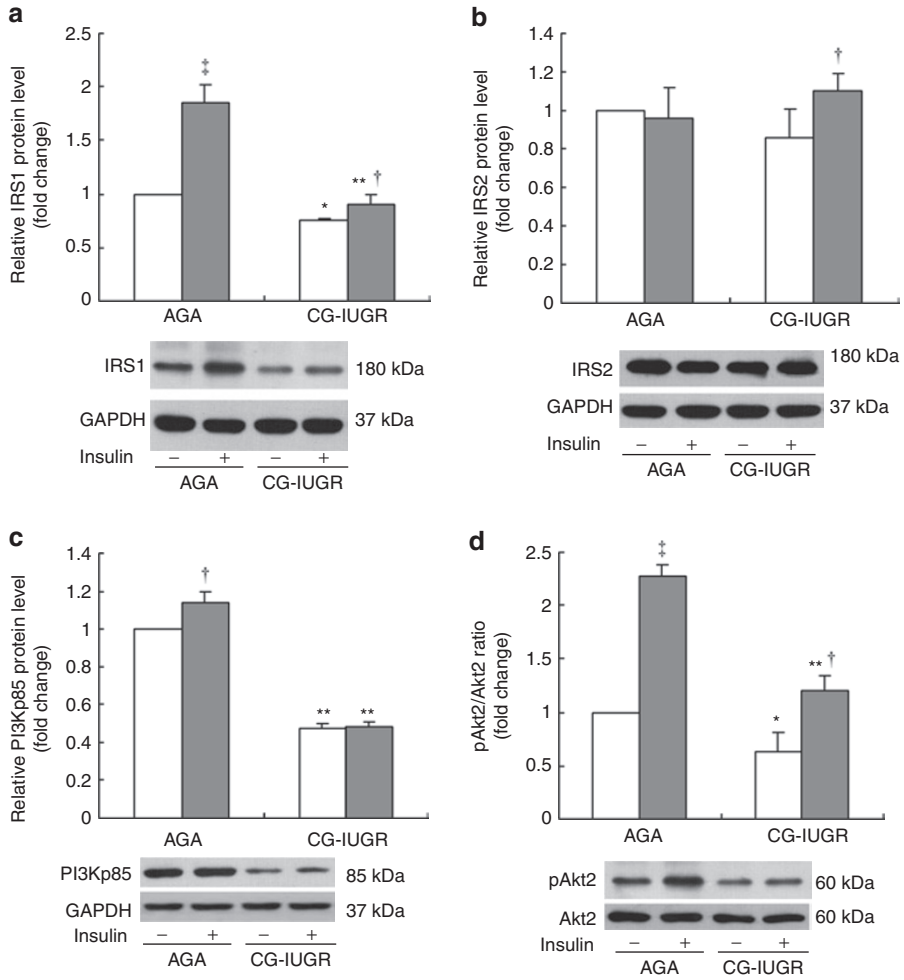

Figure 3. Relative protein levels of molecules involved in the downstream signaling of the insulin receptor. (**a**) IRS1; (**b**) IRS2; (**c**) PI3Kp85; and (**d**) phosphorylated ratios of Akt2. Representative western blots are also displayed beneath. The gray bar refers to insulin treatment, whereas the white bar indicates no insulin treatment. Data are presented as mean ± SD ($n = 6$). *$P < 0.05$ and **$P < 0.01$ CG-IUGR vs. AGA under the same condition. †$P < 0.05$ and ‡$P < 0.01$ insulin-treated vs. basal condition of the same group. AGA, appropriate for gestational age; CG-IUGR, catch-up growth intrauterine growth retardation rats; IRS, insulin receptor substrate.

hepatocytes. As shown in **Figure 6a**, the transcriptional level of PEPCK did not change significantly after the treatment with siSOCS3 in the basal state. However, after insulin stimulation, the suppression of *PEPCK* transcription was more obvious in siSOCS3-treated cells. The mRNA expression of G6Pase demonstrated a similar trend to that of PEPCK; however, the amplitude of inhibition was lower than that of the PEPCK gene (**Figure 6b**). These findings suggest that after transfection with siSOCS3, CG-IUGR cells have a reduction in hepatic glucose production due to changes in the transcriptional expression of gluconeogenesis genes.

DISCUSSION

IUGR results from a failure of the fetus to achieve its intrinsic growth potential due to anatomical or functional disorders in the feto-placental-maternal unit (16). Nutritional interventions during pregnancy have become an accepted and effective manipulation for establishing models of IUGR that attempt to mimic the nutritional situations of developing countries, where maternal malnutrition is ranked as the leading cause of IUGR (17). Furthermore, prenatal nutritional restriction has been proven to be a sensitive model for investigating the links between IUGR, early postnatal catch-up growth, and later development of metabolic disorders (18). Herein, we employed a rat model of IUGR via maternal nutritional restriction during the entire gestational period. Following enhanced nutritional supplementation after birth, the pups with IUGR exhibited catch-up growth reflected by increased fractional growth rate as compared with control animals and developed insulin resistance at 8 wk of age. The serum free fatty acid levels, which were negatively associated with insulin sensitivity in both animals and humans, trended higher in CG-IUGR rats than in controls. The fasting insulin levels in CG-IUGR rats were almost 1.7-fold higher, and the amplitudes of increased glucose and insulin levels after a glucose load were significantly higher than those of the control rats.

The liver is an insulin-sensitive organ, and many hepatic metabolic functions are coordinated by insulin. Hepatic insulin

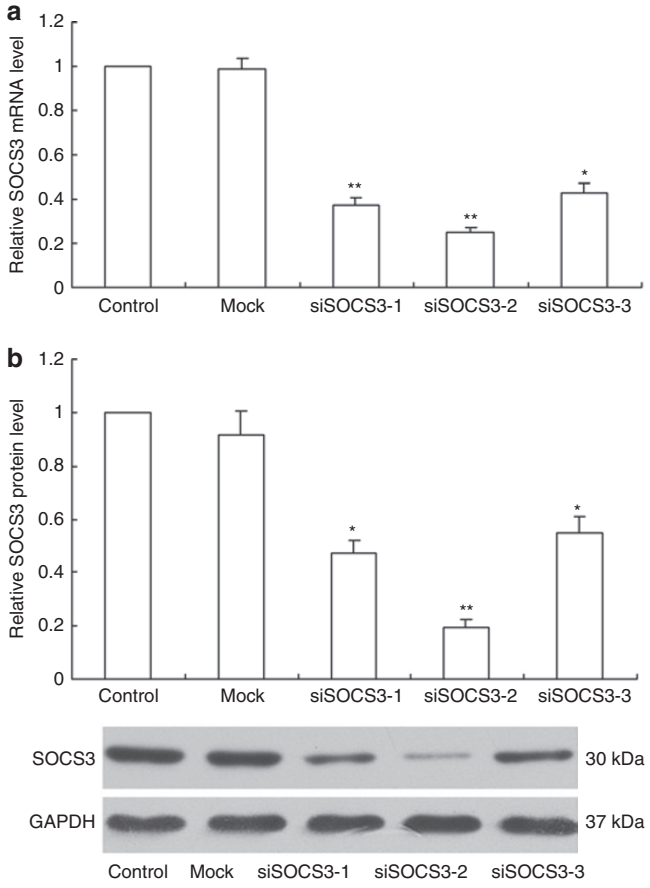

Figure 4. Relative levels of SOCS3 mRNA and protein expression in hepatocytes treated with siSOCS3. (**a**) mRNA level and (**b**) protein level and representative western blots. Data are presented as mean ± SD ($n = 3$). *$P < 0.05$ and **$P < 0.01$ vs. control hepatocytes. siSOCS3, *SOCS3*-specific small interfering RNA; SOCS3, suppressor of cytokine signaling 3.

resistance has been considered to be an underlying cause of the metabolic syndrome, nonalcoholic fatty liver, and type 2 diabetes mellitus (19). Hepatic insulin resistance is characterized by a blunted suppression of hepatic glucose production in response to insulin, which is secondary to the impairment of insulin signaling (20). A postreceptor defect in the intracellular insulin signaling cascade decreases the insulin-induced suppression of hepatic glucose production (21). IRS proteins connect activated insulin receptors with essential downstream kinase cascades, and therefore a decrease in the expression of hepatic IRS proteins may play a key role in inducing insulin resistance. Both IRS1 and IRS2 are highly expressed in the liver, and their roles in hepatic insulin action are still controversial, despite their high homology. *IRS1*-knockout mice exhibit growth retardation, insulin resistance in skeletal muscle, and glucose intolerance, whereas *IRS2*-deficient mice exhibit insulin resistance in the liver and peripheral tissues combined with impaired β-cell development, thereby leading to type 2 diabetes. In other words, IRS2 appears to play a predominant role in the insulin signaling pathway, which controls glucose metabolism (22,23). A liver-specific knockdown of *IRS1* results in an upregulation of gluconeogenesis enzymes and a trend toward elevated blood glucose levels, whereas a liver-specific knockdown of *IRS2* results in the upregulation of lipogenesis enzymes and an accumulation of lipids within the liver, suggesting that IRS1 has a major role in glucose homeostasis, whereas IRS2 is more closely related to lipid metabolism (24). In this study, we found that IRS1 levels were significantly lower in primary hepatocytes of CG-IUGR rats than in controls, whereas IRS2 expression was not different between the two groups. Following insulin stimulation, IRS protein levels were higher as compared with the basal expression levels, and IRS1 levels in the control group increased more notably than in the CG-IUGR group under insulin-stimulating conditions. These observations are consistent with the hepatic downregulation of IRS1 expression in obese mice (25). Therefore, we demonstrate that IRS1 plays a critical role in the insulin signaling pathway of primary hepatocytes isolated from CG-IUGR rats.

PI3K is a pivotal molecule activated by insulin to mediate its metabolic effects, and its p85 regulatory subunit is considered to be the main response pathway for most stimulation. Protein kinase B/Akt belongs to downstream kinases and mediates the effects of insulin on glucose transport, glycogen synthesis, protein synthesis, lipogenesis, and suppression of hepatic gluconeogenesis. The expression of both PI3K and protein kinase B is decreased in the skeletal muscle of obese patients with insulin resistance (19). Both IRS1-associated p85 levels and phosphorylated Akt expression are increased following rapamycin treatment of HepG2 cells, which display interleukin-6-induced insulin resistance (26). This observation is consistent with our findings, in which p85 levels and phosphorylated Akt2 expression were lower in CG-IUGR than AGA hepatocytes.

Accumulating evidence from human and animal studies suggests that SOCS3 may play a critical role in modulating the insulin signaling pathway. Transcriptional levels of SOCS3 were previously found to be upregulated in adipose tissue, skeletal muscle, and livers of obese mice with insulin resistance. Furthermore, an adenoviral-mediated overexpression of SOCS3 decreased the hepatic expressions of IRS1, IRS2, and PI3K, and resulted in glucose intolerance, systemic insulin resistance, and hepatic steatosis (9). Constitutive SOCS3 overexpression was also shown to decrease insulin-induced glucose uptake and lipogenesis in adipocytes (27). Therefore, we compared the expression of SOCS3 between the AGA and CG-IUGR groups, and found that SOCS3 was upregulated, whereas IRS1 and the p85 subunit of PI3K were downregulated in hepatocytes of CG-IUGR rats. These findings corroborate those of previous studies on insulin-resistant animal models. Moreover, we demonstrated that insulin could not only increase the mRNA and protein expression of SOCS3 but also that after insulin stimulation the differences in SOCS3 expression between the two groups was more obvious. Given that SOCS3 overexpression can attenuate the actions of insulin both *in vivo* and *in vitro*, it appears to be an excellent candidate for ameliorating insulin sensitivity. In this study, we found that the expressions of IRS1, the associated PI3K p85 subunit, and activated Akt2 were restored after we transfected the most effective siSOCS3 into the hepatocytes of IUGR rats. Therefore, we demonstrated that a knockdown of expression of SOCS3 can improve the transduction of the post-

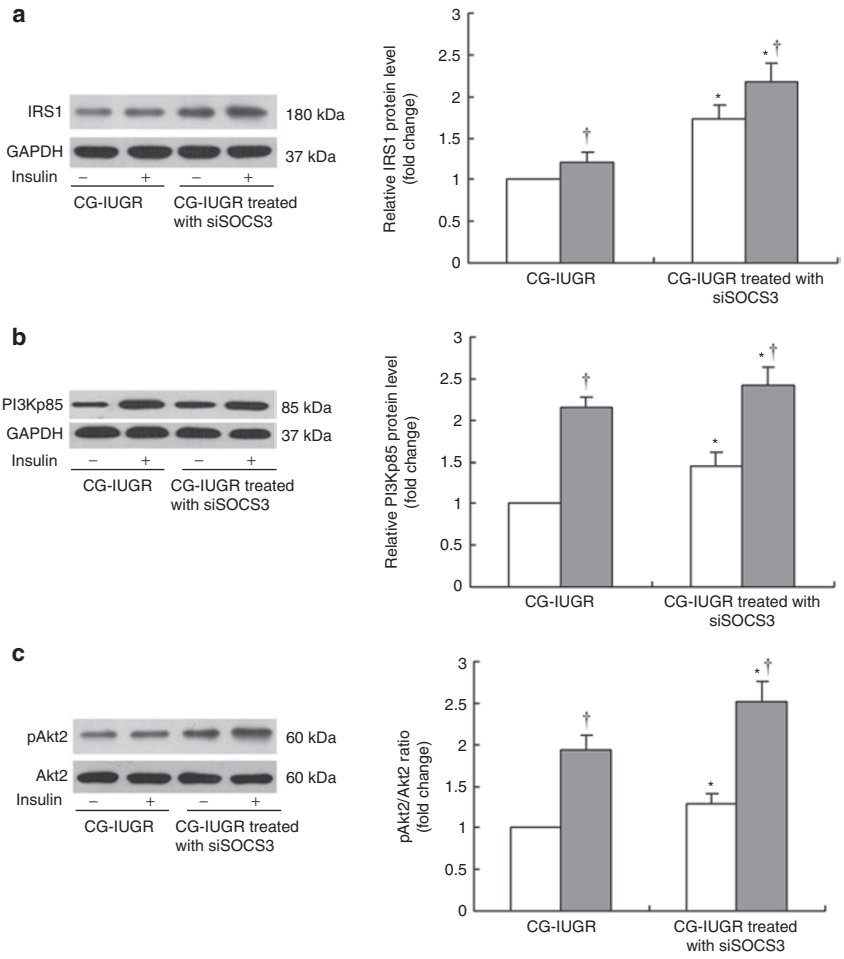

Figure 5. Relative protein expression of molecules downstream of the insulin receptor between catch-up growth IUGR rat (CG-IUGR) and siSOCS3-treated CG-IUGR hepatocytes. (**a**) IRS1; (**b**) PI3Kp85; and (**c**) phosphorylated ratios of Akt2. Representative western blots are also displayed here. The gray bar refers to insulin treatment, whereas the white bar indicates no insulin treatment. Data are presented as mean ± SD ($n = 6$). *$P < 0.05$ vs. untransfected hepatocytes of CG-IUGR rats under the same condition. †$P < 0.05$ insulin-treated vs. basal condition of the same group. IRS, insulin receptor substrate; IUGR, intrauterine growth retardation; siSOCS3, *SOCS3*-specific siRNA; SOCS3, suppressor of cytokine signaling 3.

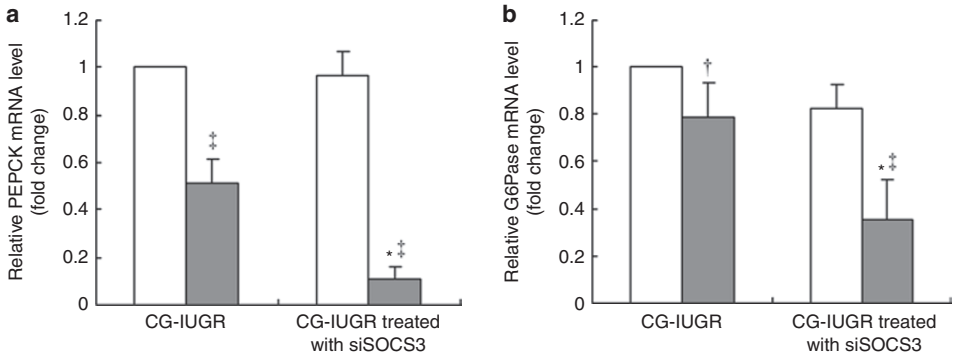

Figure 6. Relative mRNA levels of phosphoenolpyruvate carboxykinase (*PEPCK*) and glucose-6-phosphatase (*G6Pase*) genes detected via real-time PCR 48 h after selected siSOCS3 transfection. (**a**) *PEPCK* and (**b**) *G6Pase*. The gray bar refers to the insulin-treated state, whereas the white bar indicates the basal state. Data are presented as mean ± SD ($n = 6$). *$P < 0.05$ vs. CG-IUGR group under the same condition. †$P < 0.05$ and ‡$P < 0.01$ insulin-treated vs. basal condition of the same group. CG-IUGR, catch-up growth intrauterine growth retardation rats; siSOCS3, *SOCS3*-specific siRNA; SOCS3, suppressor of cytokine signaling 3.

insulin receptor signaling pathway. These findings corroborate previous study, which demonstrated that an antisense suppression of SOCS3 expression improves insulin sensitivity in the livers of obese diabetic mice (28).

PEPCK and G6Pase are the two rate-limiting enzymes in the gluconeogenesis pathway. Furthermore, G6Pase catalyzes G6P into free glucose, which is the final step shared in both gluconeogenesis and glycogenolysis. Since gluconeogenesis and glycogenolysis

result in hepatic glucose production, both enzymes have critical roles in maintaining glucose within a normal range in both the fasted and fed states. G6Pase and PEPCK expressions were previously shown to be upregulated in the livers of mice with insulin resistance or diabetes mellitus (29). This observation was consistent with the findings of our study, in which we confirmed that the mRNA levels of G6Pase and PEPCK were elevated in CG-IUGR hepatocytes as compared with controls. It was previously shown that an overexpression of G6Pase mediated by an adenovirus reduced glycogen synthesis, increased glucose production in hepatocytes, and elevated triglyceride content in skeletal muscle. In addition, it was demonstrated that basal hepatic glucose production increased in transgenic mice overexpressing PEPCK (30). Both of these genes are regulated at the transcriptional level and can be activated by peroxisome proliferative activated receptor-γ coactivator 1a (PGC-1a), which is induced by glucocorticoid and cyclic adenosine monophosphate and inhibited by insulin. In this study, after insulin stimulation, the transcriptional levels of G6Pase and PEPCK decreased in both the CG-IUGR and AGA groups. However, the amplitude of the decrease was obviously different between the two groups, indicating that the insulin signaling was blunted in the hepatocytes of CG-IUGR rats. After transfecting the effective siSOCS3 into the hepatocytes of IUGR rats, insulin sensitivity was restored and demonstrated a significantly greater downregulation in the transcriptional expressions of G6Pase and PEPCK than those without siSOCS3 treatment. Furthermore, phosphorylated Akt2 levels in CG-IUGR liver cells were elevated after transfection, and subsequently forkhead box O1 was inactivated by phosphorylation to inhibit the transcription of G6Pase and PEPCK (31). Therefore, we confirmed that knocking down the expression of SOCS3 ameliorates the insulin signaling pathway and decreases hepatic glucose production by downregulating the transcriptional expressions of gluconeogenesis genes in primary hepatocytes of CG-IUGR rats.

In summary, we employed a rat model of IUGR through maternal nutritional restriction during the entire gestational period and confirmed that primary hepatocytes from CG-IUGR rats with insulin resistance display an upregulated expression of SOCS3 and gluconeogenesis genes while downregulating the expression of molecules involved in the insulin signaling pathway. Furthermore, we demonstrated that knocking down the expression of SOCS3 improves the signal transduction of insulin through the postinsulin receptor signal pathway and ameliorates hepatic glucose metabolism through a downregulation of gluconeogenesis genes *in vitro*. Therefore, this study provides further insight into understanding the mechanism involved in the development of insulin resistance in early catch-up IUGR rats, and we speculate that targeting *SOCS3* with siRNA may be a potential therapeutic for IUGR individuals with insulin resistance, which we will investigate *in vivo* in our further study.

MATERIALS AND METHODS

Animal Model

A rat model of IUGR via maternal nutritional restriction during the entire gestational period was employed as in our previous study (15) and is briefly described as follows: Thirty female and 10 male adult rats were caged together overnight at a ratio of 3:1. Pregnant rats were randomly divided into two groups. The control group mothers (i.e., AGA group) were fed a standard rodent chow, whereas the IUGR group mothers were fed 7.5 g/d (i.e., 30% of normal intake) of the same diet from the day when pregnancy was confirmed to the day when the rat pups were delivered. Mothers in both groups were provided with food *ad libitum* following delivery. The gestation length, litter size, sex ratio, and survival rates of the fetuses were similar between the AGA and IUGR groups. The litter size was culled to five pups per litter at birth in the IUGR group, as compared with eight pups per litter in the control group, to ensure the catch-up growth of the offspring with IUGR. All pups were weaned after 3 wk of breastfeeding, and then fed a standard chow. Body weights and lengths were also measured at birth and every week thereafter. Absolute growth rate (weight gained per day) and fractional growth rate (weight gained per day, divided by birth weight) were analyzed from birth to 8 wk. Liver, skeletal muscle (right thigh), and fat pads (perirenal and retroperitoneal fat pads) were carefully dissected on rat pups aged 8 wk. Organ masses were then calculated relative to body weight and body length for standardization.

All procedures were approved by the Review Board of Animal Study Committee in Tongji Hospital, Tongji Medical College, Huazhong University of Science and Technology.

Metabolic Measurements

Eight-week-old rats were killed following a 12-h fast. Serum was separated for subsequent detection of glucose and lipid metabolism. Glucose was measured using the glucose-oxidase/peroxidase method (Rongsheng Biotech, Shanghai, China). Triglyceride, low-density lipoprotein cholesterol, high-density lipoprotein cholesterol, and total cholesterol were determined via assay kits (Huili Biotech, Changchun, China). Serum free fatty acid was assessed via a detection kit (Njjcbio, Nanjing, China). Plasma insulin was measured using an enzyme-linked immunosorbent assay kit (Millipore, Billerica, MA).

Glucose Tolerance Tests

At 8 wk of age, the offspring from both groups were fasted for 8 h. Then, after an intraperitoneal glucose injection (2 g/kg of body weight), blood was sampled from the tail vein at 0, 30, 60, 90, and 120 min.

Primary Hepatocyte Culture and Identification

Primary rat hepatocytes were isolated using a modified two-step *in situ* noncirculating perfusion method (32). The liver was perfused via the portal vein with D-Hanks buffer solution, and then again perfused with Hanks buffer solution containing 0.05% collagenase type IV (Biosharp, Seoul, South Korea). The isolated hepatocytes were washed and purified in Dulbecco's modified Eagle's medium (Hyclone, Logan, UT), filtered through a 70 μm metal mesh, and centrifuged three times at a low speed for 3 min at 39*g* at 4 °C. Cells were then resuspended in Dulbecco's modified Eagle's medium (high glucose: 22.48 mmol/l) containing 10% fetal bovine serum (Gibco, Grand Island, NY), 100 U/ml of penicillin, and 100 μg/ml of streptomycin. Cell viability was determined via Trypan blue exclusion. Hepatocytes were seeded in type I collagen-coated dishes (Sigma-Aldrich, St Louis, MO) at a density of 1×10^6 cells/cm^2 and incubated at 37 °C in a humidified atmosphere with 5% CO_2. Periodic acid Schiff staining and immunocytochemical staining targeting cytokeratin 18 (CK18) were used to identify the purity of the hepatocytes.

siSOCS3 and Transfection

Three siRNA duplexes targeting different encoding regions of rat SOCS3 and one cy3-labeled scrambled siRNA, which served as a silence negative control (Mock), were designed and chemically synthesized (Ribobio, Canton, China). The oligonucleotide sequences were as follows: siSOCS3-1 (targeting sequence: 5′-GGACCAAGAACCTACGCAT-3′), 5′-GGACCAAGAACCUACGCAUdTdT-3′ (sense), and 5′-AUGCG UAGGUUCUUGGUCCdTdT-3′ (antisense); siSOCS3-2 (targeting sequence: 5′-CCAAGAGAGCTTACTACAT-3′), 5′-CCAAGAGAGCU UACUACAUdTdT-3′ (sense), and 5′-AUGUAGUAAGCUCUCUUGG dTdT-3′ (antisense); siSOCS3-3 (targeting sequence: 5′-GGAAGACT GTCAACGGTCA-3′), 5′-GGAAGACUGUCAACGGUCAdTdT-3′ (sense), and 5′-UGACCGUUGACAGUCUUCCdTdT-3′ (antisense).

We optimized the transfection conditions to obtain the highest transfection efficiency and low cytotoxicity. Fifty nmol/l of siRNA was

transfected into hepatocytes with 5 μl of Lipofectamine 2000 reagent (Invitrogen, Carlsbad, CA) per well in a 6-well format, according to the manufacturer's protocol. Transfection efficiency was determined 4 h after transfection by dividing the number of visible fluorescent cells from the total number of corresponding cells per field and averaging across the three fields. Experiments would be subsequently performed only if the transfection effects were more than 80%. Cells were harvested 48 h after transfection to subsequently assess the silence effects.

Real-Time Quantitative PCR

Total RNA was isolated from cultured cells with TRIzol reagent (Invitrogen), according to the manufacturer's protocol. After RNA quantity and quality were assessed on an UV spectrophotometer (Eppendorf, Hamburg, Germany), RNA was reverse-transcribed into cDNA using a First Strand cDNA Synthesis Kit (Fermentas, Vilnius, Lithuania). Sequence-specific PCR primers were designed by Primer Premier 5.0 software and blasted in PubMed. All primers were synthesized by Invitrogen, and the specific details are provided in **Table 4**. Relative quantitative PCR (qPCR) was performed on an ABI 7500 real-time PCR system (Applied Biosystems, Foster City, CA). All amplifications were implemented in a total volume of 20 μl containing 50 pmol of forward and reverse primers, 250 ng of cDNA, and 10 μl of SYBR Green/ROX qPCR Master Mix (Fermentas). Melting curve analyses were carried out to verify the specificity and identity of all qPCR products. Glyceraldehyde-3-phosphate dehydrogenase was amplified as an internal control. Relative gene expression was calculated according to the comparative threshold cycle ($2^{-\Delta\Delta Ct}$) method.

Western Blotting Analysis

Cell proteins were extracted in RIPA lysis buffer containing phenylmethyl sulfonylfluoride (Beyotime, Nantong, China), and protein concentrations were measured using a BCA protein assay kit, according to the manufacturer's instructions (Beyotime, Nantong, China). Lysates containing equal protein amounts were fractionated on a 10% SDS-polyacrylamide gel and electroblotted onto nitrocellulose membranes (Millipore, Billerica, Massachusetts). After blocking with 5% nonfat milk for 1 h at room temperature, the membranes were incubated with primary antibodies (1:400 dilution for SOCS3 (Santa Cruz Biotechnology, Santa Cruz, CA); 1:600 dilution for IRS1 (Cell Signaling Technology, Danvers, MA); 1:300 dilution for IRS2 (Santa Cruz Biotechnology); 1:1,000 dilution for PI3K p85 (Cell Signaling Technology); 1:1,000 dilution for Akt2 (Cell Signaling Technology); 1:1,000 dilution for pS^{474}-Akt2 (Abcam, Cambridge, UK); 1:2,000 dilution for glyceraldehyde-3-phosphate dehydrogenase (Santa Cruz Biotechnology)) overnight at 4 °C with gentle agitation. The membranes were washed with phosphate-buffered saline containing 0.1% Tween 20 and then probed with the secondary horseradish peroxidase-conjugated antibody (Oncogene, Boston, MA) at a dilution of 1:4,000 for 1 h at room temperature. After the membranes were washed with phosphate-buffered saline containing 0.1% Tween 20 four times for 10 min each, protein bands were visualized using the enhanced chemiluminescence detection kit (Thermo Scientific, Rockford, IL). The same membranes were stripped and reprobed with phospho-specific antibodies to detect the levels of phosphorylated proteins. Semi-quantification of protein bands was evaluated by densitometry using a UVP BioSpectrum imaging system (UVP, Upland, CA).

Table 4. The primers used in qPCR

Gene	Primer	Sequence from 5′→3′	Product length
SOCS3	Forward	GGGACCAAGAACCTACGC	187 bp
	Reverse	GCTGCTCCTGAACCTCAAA	
IRS1	Forward	CGCTACATCCCAGGTGC	113 bp
	Reverse	GTGCCAGCCGAGTGAGT	
IRS2	Forward	GCGGACGCCAAGCACAA	128 bp
	Reverse	CGGCCTTCGCTGACCAA	
PI3K	Forward	GAGGTGCTCTGGAATGT	204 bp
	Reverse	GAGGAAGCGGTGGTCTA	
AKT2	Forward	AAGGCTGGCTCCACAAAC	195 bp
	Reverse	CAAAGGTGTTGGGTCGTG	
PEPCK	Forward	GCTCACTCCCATTGGCTACG	144 bp
	Reverse	TGGTCCTCCAGATACTTGTCG	
G6Pase	Forward	GACCTCAGGAACGCCTTCTATGT	185 bp
	Reverse	ACGGAGCTGTTGCTGTAATAGTCA	
GAPDH	Forward	GCACAGTCAAGGCTGAGAATG	140 bp
	Reverse	GGTGGTGAAGACGCCAGTA	

GAPDH, glyceraldehyde-3-phosphate dehydrogenase; G6Pase, glucose-6-phosphatase; IRS, insulin receptor substrate; SOCS3, suppressor of cytokine signaling 3; PEPCK, phosphoenolpyruvate carboxykinase; PI3K, phosphatidylinositol 3-kinase.

Statistical Analysis

All data were presented as mean ± SD. Differences between two groups were evaluated by an independent-sample *t*-test, and comparisons between three or more groups were performed by an ANOVA. Statistical analyses were performed using SPSS 15.0 software (SPSS, Chicago, IL), and differences were considered statistically significant when the *P* value was <0.05.

STATEMENT OF FINANCIAL SUPPORT

This study was supported by the National Natural Science Foundation of China (grants 30772358 and 81170627).

REFERENCES

1. Morrison JL, Duffield JA, Muhlhausler BS, Gentili S, McMillen IC. Fetal growth restriction, catch-up growth and the early origins of insulin resistance and visceral obesity. Pediatr Nephrol 2010;25:669–77.
2. Neitzke U, Harder T, Plagemann A. Intrauterine growth restriction and developmental programming of the metabolic syndrome: a critical appraisal. Microcirculation 2011;18:304–11.
3. Kanaka-Gantenbein C. Fetal origins of adult diabetes. Ann N Y Acad Sci 2010;1205:99–105.
4. Valsamakis G, Kanaka-Gantenbein C, Malamitsi-Puchner A, Mastorakos G. Causes of intrauterine growth restriction and the postnatal development of the metabolic syndrome. Ann N Y Acad Sci 2006;1092:138–47.
5. Soto N, Bazaes RA, Peña V, et al. Insulin sensitivity and secretion are related to catch-up growth in small-for-gestational-age infants at age 1 year: results from a prospective cohort. J Clin Endocrinol Metab 2003;88:3645–50.
6. Krebs DL, Hilton DJ. SOCS: physiological suppressors of cytokine signaling. J Cell Sci 2000;113 (Pt 16):2813–9.
7. Emanuelli B, Peraldi P, Filloux C, et al. SOCS-3 inhibits insulin signaling and is up-regulated in response to tumor necrosis factor-alpha in the adipose tissue of obese mice. J Biol Chem 2001;276:47944–9.
8. Ueki K, Kondo T, Kahn CR. Suppressor of cytokine signaling 1 (SOCS-1) and SOCS-3 cause insulin resistance through inhibition of tyrosine phosphorylation of insulin receptor substrate proteins by discrete mechanisms. Mol Cell Biol 2004;24:5434–46.
9. Lebrun P, Van Obberghen E. SOCS proteins causing trouble in insulin action. Acta Physiol (Oxf) 2008;192:29–36.
10. Laubner K, Kieffer TJ, Lam NT, Niu X, Jakob F, Seufert J. Inhibition of preproinsulin gene expression by leptin induction of suppressor of cytokine signaling 3 in pancreatic beta-cells. Diabetes 2005;54:3410–7.
11. Howard JK, Cave BJ, Oksanen LJ, Tzameli I, Bjørbaek C, Flier JS. Enhanced leptin sensitivity and attenuation of diet-induced obesity in mice with haploinsufficiency of Socs3. Nat Med 2004;10:734–8.
12. Marine JC, McKay C, Wang D, et al. SOCS3 is essential in the regulation of fetal liver erythropoiesis. Cell 1999;98:617–27.
13. Torisu T, Sato N, Yoshiga D, et al. The dual function of hepatic SOCS3 in insulin resistance in vivo. Genes Cells 2007;12:143–54.
14. Gu H, Liu L, Ma S, et al. Inhibition of SOCS-3 in adipocytes of rats with diet-induced obesity increases leptin-mediated fatty acid oxidation. Endocrine 2009;36:546–54.

15. Liao L, Zheng R, Wang C, et al. The influence of down-regulation of suppressor of cellular signaling proteins by RNAi on glucose transport of intrauterine growth retardation rats. Pediatr Res 2011;69:497–503.
16. Wollmann HA. Intrauterine growth restriction: definition and etiology. Horm Res 1998;49:Suppl 2:1–6.
17. Vuguin PM. Animal models for small for gestational age and fetal programming of adult disease. Horm Res 2007;68:113–23.
18. Shahkhalili Y, Moulin J, Zbinden I, Aprikian O, Macé K. Comparison of two models of intrauterine growth restriction for early catch-up growth and later development of glucose intolerance and obesity in rats. Am J Physiol Regul Integr Comp Physiol 2010;298:R141–6.
19. Meshkani R, Adeli K. Hepatic insulin resistance, metabolic syndrome and cardiovascular disease. Clin Biochem 2009;42:1331–46.
20. Vuguin P, Raab E, Liu B, Barzilai N, Simmons R. Hepatic insulin resistance precedes the development of diabetes in a model of intrauterine growth retardation. Diabetes 2004;53:2617–22.
21. Barthel A, Schmoll D. Novel concepts in insulin regulation of hepatic gluconeogenesis. Am J Physiol Endocrinol Metab 2003;285:E685–92.
22. Withers DJ, Gutierrez JS, Towery H, et al. Disruption of IRS-2 causes type 2 diabetes in mice. Nature 1998;391:900–4.
23. Saltiel AR, Kahn CR. Insulin signalling and the regulation of glucose and lipid metabolism. Nature 2001;414:799–806.
24. Taniguchi CM, Ueki K, Kahn R. Complementary roles of IRS-1 and IRS-2 in the hepatic regulation of metabolism. J Clin Invest 2005;115:718–27.
25. Standaert ML, Sajan MP, Miura A, et al. Insulin-induced activation of atypical protein kinase C, but not protein kinase B, is maintained in diabetic (ob/ob and Goto-Kakazaki) liver. Contrasting insulin signaling patterns in liver versus muscle define phenotypes of type 2 diabetic and high fat-induced insulin-resistant states. J Biol Chem 2004;279:24929–34.
26. Kim JH, Kim JE, Liu HY, Cao W, Chen J. Regulation of interleukin-6-induced hepatic insulin resistance by mammalian target of rapamycin through the STAT3-SOCS3 pathway. J Biol Chem 2008;283:708–15.
27. Shi H, Cave B, Inouye K, Bjørbaek C, Flier JS. Overexpression of suppressor of cytokine signaling 3 in adipose tissue causes local but not systemic insulin resistance. Diabetes 2006;55:699–707.
28. Ueki K, Kondo T, Tseng YH, Kahn CR. Central role of suppressors of cytokine signaling proteins in hepatic steatosis, insulin resistance, and the metabolic syndrome in the mouse. Proc Natl Acad Sci USA 2004;101:10422–7.
29. Michael MD, Kulkarni RN, Postic C, et al. Loss of insulin signaling in hepatocytes leads to severe insulin resistance and progressive hepatic dysfunction. Mol Cell 2000;6:87–97.
30. Postic C, Dentin R, Girard J. Role of the liver in the control of carbohydrate and lipid homeostasis. Diabetes Metab 2004;30:398–408.
31. Cheng Z, White MF. Targeting Forkhead box O1 from the concept to metabolic diseases: lessons from mouse models. Antioxid Redox Signal 2011;14:649–61.
32. Seglen PO. Preparation of isolated rat liver cells. Methods Cell Biol 1976;13:29–83.